count for the observed products in terms of a heterolytic metal–metal bond scission can be written as shown in eq 24–28. Reaction of $Mn(CO)_5py^+$ in neat pyridine to form

$$Mn_2(CO)_{10} \overset{h\nu}{\rightleftharpoons} Mn(CO)_5^+ + Mn(CO)_5^- \quad (24)$$

$$Mn(CO)_5^+ + py \rightarrow Mn(CO)_5py^+ \quad (25)$$

$$Mn(CO)_5py^+ \rightarrow Mn(CO)_4py^+ + CO \quad (26)$$

$$Mn(CO)_4py^+ + Mn(CO)_5^- \rightarrow Mn_2(CO)_9py \quad (27)$$

$$Mn(CO)_5py^+ + 2py \rightarrow Mn(CO)_3(py)_3^+ + 2CO \quad (28)$$

$Mn(CO)_3(py)_3^+$ is very rapid at room temperature.[15] To form $Mn_2(CO)_9py$ in significant amounts would therefore require an overall very rapid rate for processes 26 and 27. We have studied the reaction of $[Mn(CO)_5py^+]BF_4^-$ with $[(C_6H_5)_6P_2N^+][Mn(CO)_5^-]$ in pyridine. The sole product observed is $[Mn(CO)_3(py)_3^+][Mn(CO)_5^-]$; no evidence for $Mn_2(CO)_9py$ was seen in the IR spectra of the reaction mixture. Further evidence of homolysis of the metal–metal bond in the photochemical reaction comes from the results obtained when CCl_4 is present upon photolysis of $Mn_2(CO)_9py$, as described above. It is difficult to see how the observed products could be accounted for on the basis of a heterolytic cleavage of the metal–metal bond.

The mechanism we have presented here is applicable to the disproportionation reactions of other dinuclear metal carbonyl compounds in donor solvents such as THF, amines, and so forth[41-47] and may apply also the photochemical reactions of $(\eta^5\text{-}C_5H_5)_2Mo_2(CO)_6$ with halides and phosphines, in which ionic products are observed.[48-50]

(43) Herberhold, M.; Wehrmann, F.; Neugebauer, D.; Huttner, G. *J. Organomet. Chem.* **1978**, *152*, 329.
(44) Sternberg, H. W.; Wender, I.; Friedel, R. A.; Orchin, M. *J. Am. Chem. Soc.* **1953**, *75*, 3148.
(45) Hieber, W.; Sedlmeier, J.; Abeck, W. *Chem. Ber.* **1953**, *86*, 700.
(46) Hieber, W.; Sedlmeier, J. *Chem. Ber.* **1954**, *87*, 25.
(47) Hieber, W.; Weisboeck, R. *Chem. Ber.* **1958**, *88*, 91.
(48) Burkett, A. R.; Meyer, T. J.; Whitten, D. G. *J. Organomet. Chem.* **1974**, *67*, 67.
(49) Hughey, J. L. Ph.D. Thesis, The University of North Carolina, 1975.
(50) Haines, R. J.; Nyholm, R. S.; Stiddard, M. H. B. *J. Chem. Soc. A* **1968**, *43*.

Contribution from the Department of Chemistry, University of Minnesota, Minneapolis, Minnesota 55455

Synthesis and Reactivity of an Anionic Tetrairon Nitrido Cluster. Crystal and Molecular Structure of $PPN[Fe_4N(CO)_{12}]$

DOUGLAS E. FJARE and WAYNE L. GLADFELTER*

Received March 10, 1981

The reaction of $PPN[Fe(CO)_3(NO)]$ (PPN = bis(triphenylphosphin)iminium cation) with $Fe_3(CO)_{12}$ produces the nitrido cluster $PPN[Fe_4N(CO)_{12}]$. The structure was determined by single-crystal X-ray crystallography [$P\bar{1}$ space group, Z = 2, a = 10.700 (2) Å, b = 14.146 (3) Å, c = 16.249 (3) Å, α = 91.15 (1)°, β = 94.55 (2)°, γ = 97.52 (2)°] and found to contain a butterfly arrangement of iron atoms with the nitrogen situated in the center of the cluster. $[Fe_4N(CO)_{12}]^-$ reacts with acids giving several products, of which $Fe_4N(CO)_{12}H$ is the major derivative. The remaining products, apparently formed when excess acid and free carbon monoxide are present, are $Fe_4N(CO)_{11}(NO)$, $Fe_3(NH)(CO)_{10}$, and $Fe_3(NH)_2(CO)_9$. The last two imido clusters have been characterized by comparison to existing related compounds. The structure of $Fe_4N(CO)_{11}(NO)$ likely contains the same Fe_4N moiety as $[Fe_4N(CO)_{12}]^-$, although other structures are possible. The reaction of $NOPF_6$ with $PPN[Fe_4N(CO)_{12}]$ produces $Fe_4N(CO)_{11}(NO)$ in 62% yield.

Introduction

The ability of metal clusters to bind, stabilize, and/or activate small molecules has led to several fascinating discoveries. The synthesis and characterization of new functional groups such as C_2,[1] η^2-CH,[2] and η^2-CO,[3] as well as cluster-bound atomic species of C,[4] P,[5] S,[6] and N,[7-9] are providing some insight into the chemistry that occurs on metal surfaces. Nitrido clusters are a recent development in this area.[7-9] Martinengo and co-workers[7] prepared the first example of nitrido clusters with low valent metals using the reaction of $NOBF_4$ with $[Co_6(CO)_{15}]^{2-}$ forming $[Co_6N(CO)_{15}]^-$ (I) in

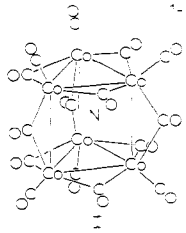

40–50% yield. Muetterties and co-workers[8] utilized this nitrosonium ion approach and conducted the reaction of $NOBF_4$ with a mixture of $[Fe_2(CO)_8]^{2-}$ and $Fe(CO)_5$ at 130 °C for 1 h. The tetrairon nitride $[Fe_4N(CO)_{12}]^-$ was isolated from

(1) Albano, V. G.; Chini, P.; Martinengo, S.; Sansoni, M.; Strumolo, D. *J. Chem. Soc., Dalton Trans.* **1978**, 459–463.
(2) (a) Tachikawa, M.; Muetterties, E. L. *J. Am. Chem. Soc.* **1980**, *102*, 4541–4542. (b) Beno, M. A.; Williams, J. M.; Tachikawa, M.; Muetterties, E. L. *Ibid.* **1980**, *102*, 4542–4544.
(3) Manassero, M.; Sansoni, M.; Longoni, G. *J. Chem. Soc., Chem. Commun.* **1976**, 919–921.
(4) Chini, P.; Longoni, G.; Albano, V. G. *Adv. Organomet. Chem.* **1976**, *14*, 285–344.
(5) Vidal, J. L.; Walker, W. E.; Pruett, R. L.; Schoening, R. C. *Inorg. Chem.* **1979**, *18*, 129–136.
(6) Vidal, J.; Fiato, R. A.; Cosby, L. A.; Pruett, R. L. *Inorg. Chem.* **1978**, *17*, 2574–2582.
(7) Martinengo, S.; Ciani, G.; Sironi, A.; Heaton, B. T.; Mason, J. *J. Am. Chem. Soc.* **1979**, *101*, 7095–7097.
(8) Tachikawa, M.; Stein, J.; Muetterties, E. L.; Teller, R. G.; Beno, M. A.; Gebert, E.; Williams, J. M. *J. Am. Chem. Soc.* **1980**, *102*, 6648–6649.
(9) Fjare, D. E.; Gladfelter, W. L. *J. Am. Chem. Soc.* **1981**, *103*, 1572–1574.

0020-1669/81/1320-3533$01.25/0

this mixture in 3.3% yield. Longer reaction times resulted in the formation of $[Fe_5N(CO)_{14}]^-$, in 66% yield, which was protonated to give $Fe_5N(CO)_{14}H$ (II). We have discovered[9] that $[Fe_4N(CO)_{12}]^-$ can be readily prepared by a reaction which does not involve ^+NO as a reagent.

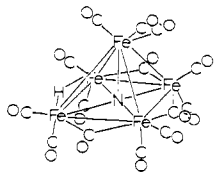

II

Transition-metal nitrides of high valent metals, on the other hand, have long been known.[10] Mononuclear examples such as $[Os(N)(O)_3]^-$ have a metal–nitrogen triple bond. Doubly bridging examples such as Os_2N(dithiocarbamato)$_5$[11] have linear Os–N–Os interactions; and in $[Ir_3N(SO_4)_6(H_2O)_3]^{6-}$, the nitrogen is bound in the center of an equilateral triangle of metal atoms.

In light of the metal cluster–metal surface analogy,[12] the low-valent nitrido clusters are particularly interesting. Several surface reactions involving NO or N_2 are known to occur via an adsorbed nitrogen atom. In the case of the Haber process, the mechanism is believed to occur via formation of the metal nitride followed by successive addition of hydrogen atoms to the nitrogen giving ammonia.[13] In this paper we will present our synthesis of $[Fe_4N(CO)_{12}]^-$, as mentioned above, the results of a single-crystal X-ray crystallographic study, and the protonation of $[Fe_4N(CO)_{12}]^-$ which gives several products including some having N–H bonds.

Experimental Section

$Fe_3(CO)_{12}$,[14] Na[$Fe(CO)_3(NO)$],[15] and PPN[$Fe(CO)_3(NO)$][16] (PPN = bis(triphenylphosphin)iminium cation) were prepared according to published procedures. Tetrahydrofuran (THF) and diethyl ether were dried by distillation from sodium benzophenone ketyl under N_2. Methanol was dried by distillation from $Mg(OMe)_2$. All other solvents were used as obtained. All reactions were carried out under an N_2 atmosphere which was maintained either up to the point of the first hexane extraction following acidification in the preparation of neutral compounds or until the formation of crystals of the salts was complete. Chromatography was conducted on silica gel.

Preparation of PPN[$Fe_4N(CO)_{12}$]. $Fe_3(CO)_{12}$ (1.52 g, 3.02 mmol) was dissolved in 125 mL of THF and cooled at −78 °C. PPN[$Fe(CO)_3(NO)$] (1.42 g, 2.00 mmol) was dissolved in 50 mL of THF and added by syringe to the $Fe_3(CO)_{12}$ solution. The reaction commenced when the temperature reached −15 °C, and the solution was stirred at room temperature for 10 h. The THF was removed under vacuum and the residue dissolved in 75 mL of diethyl ether and filtered. The diethyl ether was then removed under vacuum, and 40 mL of ethanol was added. This volume was slowly reduced to 15 mL by evaporation under vacuum to give black air-stable crystals of PPN[$Fe_4N(CO)_{12}$] in 50% yield (1.12 g, 1.01 mmol). Anal. Calcd for PPN[$Fe_4N(CO)_{12}$]: C, 51.84; H, 2.72; N, 2.52. Found: C, 51.62; H, 2.79; N, 2.53.

Protonation of PPN[$Fe_4N(CO)_{12}$]. To PPN[$Fe_4N(CO)_{12}$] (104.9 mg, 0.094 mmol) in 10 mL of dry, deoxygenated CH_2Cl_2 at −78 °C was added 9.4 μL of CF_3SO_3H. TLC of the solution indicated only one product. The solvent was removed under vacuum and the residue extracted into hexane. Evaporation of the hexane gave 49.8 mg (92% yield) of black air-stable microcrystalline product. An infrared and mass spectrum of the product confirmed its identity as $Fe_4N(CO)_{12}H$.

Table I

Crystal Parameters	
crystal system = triclinic	V = 2429 (2) Å^3
space group = $P\bar{1}$	Z = 2
a = 10.700 (2) Å	calcd density = 1.54 g/cm^3
b = 14.146 (3) Å	temp = 22 °C
c = 16.249 (3) Å	abs coeff = 13.31 cm^{-1}
α = 91.15 (1)°	formula = $C_{48}H_{30}Fe_4N_2O_{12}P_2$
β = 94.55 (2)°	
γ = 97.52 (2)°	

Measurement of Intensity Data

diffractometer: Enraf-Nonius CAD4
radiation: Mo Kα (λ = 0.710 69 Å)
monochromator: graphite crystal
scan speed: variable, from 3.17 to 20.00°/min
scan range: $0° \leq 2\theta \leq 50°$
reflctns measd: $+h, \pm k, \pm l$
check reflctns: {−6,−2,2}, {−2,−1,9}, {−2,−7,−1}; measd approximately every 150 reflctns
reflctns collected: 8544 unique reflctns; 4001 with $I > 2.0\sigma(I)$
p = 0.03
R = 0.054
R_w = 0.051

Synthesis and Protonation of Na[$Fe_4N(CO)_{12}$]. A 50-mL THF solution of Na[$Fe(CO)_3(NO)$] (1.05 g, 5.44 mmol) was added dropwise over 10 min to a stirred 100-mL solution of $Fe_3(CO)_{12}$ (2.652 g, 5.27 mmol). Upon addition, the color immediately began changing from green to dark brown, and after 20 min the infrared spectrum indicated complete consumption of $Fe_3(CO)_{12}$. The solvent was immediately evaporated under vacuum. Hexane (100 mL) was deoxygenated by an N_2 purge and added to the residue, followed by addition of 25 mL of deoxygenated 20% H_3PO_4. The hexane remained colorless until addition of the acid, when it became dark brown. The two layers were separated with a separatory funnel, and the acid layer was extracted with hexane until colorless. The hexane layers were dried over anhydrous $MgSO_4$ and filtered. TLC analysis indicated the presence of several minor products. After the solvent and any $Fe(CO)_2(NO)_2$ were removed by evaporation, the crystals were washed with three 25-mL portions of hexane. This removed all of the low-yield products except some $Fe_4N(CO)_{11}(NO)$. Repeated recrystallization from CH_2Cl_2 by slow cooling gave pure $Fe_4N(CO)_{12}H$ in 43% yield (1.31 g). The remaining products (from the washings) were separated by column chromatography, with hexane as the eluant. The first fraction off the column was brown $Fe_4N(CO)_{11}(NO)$, which was collected in 5.5% yield (168 mg). Anal. Calcd for $Fe_4N(CO)_{11}(NO)$: C, 22.95; N, 4.87. Found: C, 23.12; N, 4.66. Immediately following this was green $Fe_3(CO)_{12}$. Next to elute was a light peach-colored band. Only a trace amount has been isolated, and the formulation of this compound is suggested to be $Fe_3(NH)_2(CO)_9$ by mass spectroscopy. (Parent ion m/e 450, followed by loss of nine carbonyls to a very strong peak at m/e 198, due to $Fe_3(NH)_2^+$.) Two very slow bands were stripped from the column with CH_2Cl_2/hexane. The first is green and has not been characterized. The second is red $Fe_3(NH)(CO)_{10}$, collected in 3.0% yield (73 mg) based on $Fe_3(CO)_{12}$. Anal. Calcd for $Fe_3(NH)(CO)_{10}$: C, 25.96; H, 0.22; N, 3.03. Found: C, 25.80; H, 0.20; N, 3.03.

Detection of CO_2. $Fe_3(CO)_{12}$ (187 mg, 0.371 mmol) and PPN[$Fe(CO)_3(NO)$] (163 mg, 0.230 mmol) were placed in a reaction vessel. Dichloromethane was distilled into the vessel under vacuum, and the reaction vessel was sealed. After the reaction appeared to be complete, the solution was cooled to −78 °C. The tube was opened to the mass spectrometer (AEI MS30), and the peak at m/e 44 was observed.

Reaction of PPN[$Fe_4N(CO)_{12}$] with $NOPF_6$. PPN[$Fe_4N(CO)_{12}$] (119.7 mg, 0.108 mmol) and $NOPF_6$ (21.2 mg, 0.122 mmol) were placed in a Schlenk flask, and 20 mL of dry, deoxygenated CH_2Cl_2 was distilled into the flask under reduced pressure. The solution was allowed to warm to room temperature, and the reaction was stopped when the infrared spectrum indicated complete consumption of PPN[$Fe_4N(CO)_{12}$] (~15 min). The solution was filtered, and the solvent was removed on a rotary evaporator and extracted into hexane

(10) Griffith, W. P. *Coord. Chem. Rev.* **1972**, *8*, 369–396.
(11) Given, K. W.; Pignolet, L. H. *Inorg. Chem.* **1977**, *16*, 2982–2984.
(12) Muetterties, E. L.; Rhodin, T. N.; Bard, E.; Brucker, C. F.; Pretzer, W. R. *Chem. Rev.* **1979**, *79*, 91–137.
(13) Emmett, P. H. "The Physical Basis for Heterogeneous Catalysis"; Drauglis, E., Jaffe, R. I., Eds.; Plenum Press: New York, 1975; pp 3–34.
(14) McFarlane, W.; Wilinson, G. *Inorg. Synth.* **1966**, *8*, 181–183.
(15) Beutner, H.; Hieber, W. *Z. Naturforsch. B: Anorg. Chem., Org. Chem., Biochem., Biophys., Biol.* **1960**, *156*, 323–324.
(16) Connelly, N. G.; Gardner, C. *J. Chem. Soc., Dalton Trans.* **1976**, 1525–1527.

to give 38.3 mg (62% yield) of black microcrystalline $Fe_4N(CO)_{11}(NO)$.

Collection and Reduction of the X-ray Data. Black crystals of $PPN[Fe_4N(CO)_{12}]$ were grown from a solution of ether/hexane; one of which was mounted on a glass fiber. The crystal was found to be triclinic by the Enraf-Nonius CAD4-SDP peak search, centering, and indexing programs, and by a Delaney reduction calculation.[17] The centrosymmetric space group $P\bar{1}$ was chosen and data collection begun. Successful refinement of the structure verified the choice of this space group. A summary of the crystal data is presented in Table I. Background counts were measured at both ends of the scan range with the use of a ω-2θ scan, equal at each side to one-fourth of the scan range of the peak. In this manner, the total duration of measuring background is equal to half of the time required for the peak scan. The three check reflections showed no change in intensity during data collection. A total of 8544 unique reflections were measured, of which 4001 had $I > 2.0\sigma I$, and were used in the structural determination.[18] The data were corrected for Lorentz, polarization, and background effects but not for adsorption.

Solution and Refinement of the Structure. The structure was solved by conventional heavy-atom techniques. The positions of the four iron atoms were determined by a Patterson synthesis. Subsequent structure factor and difference Fourier calculations revealed the positions of the nonhydrogen atoms.[19] All atoms in the cluster and the P and N atoms in the cation were refined with the use of anisotropic temperature factors. The hydrogen atom positions were calculated and used in the calculations, but their positions and temperature factors [set by $B(H) = B(C) + 1.0$] were not refined. The values of the atomic scattering factors used in the calculations were taken from the usual tabulation,[20] and the effects of anomalous dispersion were included for the nonhydrogen atoms. The hydrogen atom scattering factors were taken from Cromer and Ibers' list.[21] After convergence was reached, a review of the temperature factors revealed no unusual features. A check was performed at this point to prove that the central atom was nitrogen rather than carbon. After replacement, three cycles of least-squares refinement caused the unweighted R factor to increase to 0.056 and, more importantly, the isotropic equivalent temperature factor of this atom to drop to 2.053 from its value of 3.728 as a nitrogen. These features support the assignment of the core atom to nitrogen.

Results

Synthesis of $[Fe_4N(CO)_{12}]^-$. The reaction of $PPN[Fe(CO)_3NO]$ with $Fe_3(CO)_{12}$ occurs readily at room temperature. Infrared spectroscopic monitoring of the reaction indicates that the optimum stoichiometry requires 1.5 equiv of $Fe_3(CO)_{12}$ for each equivalent of $[Fe(CO)_3(NO)]^-$. The products of the reaction were determined to be $[Fe_4N(CO)_{12}]^-$, $Fe(CO)_5$, CO_2, and CO. The number of equivalents of $Fe(CO)_5$ produced was quantitatively analyzed by ultraviolet spectroscopy and found to be 1.5 times the value for $[Fe(CO)_3(NO)]^-$ (Table V). This information is consistent with the stoichiometry shown in eq 1. Although this reaction appears to be clean

$$3Fe_3(CO)_{12} + 2PPN[Fe(CO)_3(NO)] \rightarrow 2PPN[Fe_4N(CO)_{12}] + 3Fe(CO)_5 + 2CO_2 + CO \quad (1)$$

and quantitative by spectroscopic measurements, we have never obtained high recrystallized yields of $PPN[Fe_4N(CO)_{12}]$. We believe this is mainly due to difficulties in the crystallization itself, which gives a 50% yield.

The reaction is similar when Na^+ is used in place of the PPN^+ salt. Although $Na[Fe_4N(CO)_{12}]$ was never isolated, the infrared spectrum of the reaction mixture is virtually identical with that resulting from the $PPN[Fe(CO)_3(NO)]$ reaction (Table VI).

Protonation of $[Fe_4N(CO)_{12}]^-$. When a stoichiometric quantity of CF_3SO_3H is added to a CH_2Cl_2 solution of $PPN[Fe_4N(CO)_{12}]$, protonation occurs brown). after solvent removal, black crystals (its color in solution is dark brown. Mass spectrometric and elemental analyses suggest the formula is $Fe_4N(CO)_{12}H$. The ^1H NMR spectrum exhibits a signal at δ −31.2 in $CDCl_3$, suggesting protonation occurs on one of the iron–iron bonds. The infrared spectrum shows no evidence of low-energy bands that might be due to bridging carbonyl and/or terminal or bridging nitrosyl ligands.

As discussed above, the reaction of $Na[Fe(CO)_3(NO)]$ with $Fe_3(CO)_{12}$ produces $Na[Fe_4N(CO)_{12}]$. This can be protonated with aqueous mineral acids such as H_3PO_4. The main product is $Fe_4N(CO)_{12}H$, which is isolated in 43% yield. Unlike the nonaqueous protonation, however, other products were obtained which were separated with the use of silica gel chromatography. The second most abundant fraction is a black microcrystalline species which has a parent ion in the mass spectrum at m/e 576 (compared to m/e 575 for $Fe_4N(CO)_{12}H$). No signals were observed in the ^1H NMR spectrum, and the infrared spectrum (Figure 4) appears to be similar to those of the other nitrido clusters except for the peak at 1791 cm^{-1}. The elemental analysis suggests two nitrogens are present, and the formulation consistent with the mass spectrum is $Fe_4N(CO)_{11}(NO)$. This cluster has also been prepared in a more rational fashion by the reaction of $NOPF_6$ with $PPN[Fe_4N(CO)_{12}]$ in 62% yield.

A red compound which was obtained in very low (3%) yield has been characterized as $Fe_3(NH)(CO)_{10}$ by mass spectrometric and elemental analysis. The infrared is relatively simple, indicating a higher symmetry structure. There is a low-energy band at 1749 cm^{-1} indicative of a bridging carbonyl or a terminal nitrosyl ligand. The ^1H NMR spectrum is particularly informative, as a 1:1:1 multiplet occurs at δ +9.4 with a coupling constant of 57 Hz. This is strong evidence that the compound has a N–H group present. The observation of a weak peak at 3368 cm^{-1} in the ν_{N-H} region of the infrared supports this assignment.

Another red compound obtained is related to the above species. $Fe_3(NH)_2(CO)_9$ is isolated in only trace yield, and we only have mass spectrometric and infrared evidence for its characterization.

X-ray Crystallographic Analysis of $PPN[Fe_4N(CO)_{12}]$. An overview of the structure is seen in the stereoview in Figure 1, and the labeling sequence is shown in Figure 2. The overall symmetry of the molecule conforms closely to the point group C_{2v}. The deviations which are observed involve a small (~3–4°) twist of the Fe(1) and Fe(2) tricarbonyl groups such that they are equivalent only under the twofold rotation axis. Quantitatively, this can be seen in a comparison of the Fe(2)–Fe(1)–C(11) angle of 95.4 (2)° and the Fe(2)–Fe(1)–C(13) angle of 99.2 (2)°. The analogous angles about Fe(2) are Fe(1)–Fe(2)–C(23), which is 97.5 (2)°, and Fe(1)–Fe(2)–C(21), which is 101.7 (2)°. These values further show

(17) All calculations were carried out on PDP 8A and 11/34 computers using the Enraf-Nonius CAD 4-SDP programs. This crystallographic computing package is described in: Frenz, B. A. In "Computing in Crystallography"; Schenk, H., Olthof-Hazekamp, R., van Koningsveld, H., Bassi, G. C., Eds.; Delft University Press: Delft, Holland, 1978; pp 64–71. See also: "CAD 4 and SDP Users Manual"; Enraf-Nonius: Delft, Holland, 1978.

(18) The intensity data were processed as described: "CAD 4 and SDP User's Manual"; Enraf-Nonius: Delft, Holland, 1978. The net intensity $I = (K/\text{NPI})(C - 2B)$, where $K = 20.1166x$ (attenuator factor). NPI = ratio of fastest possible scan rate to scan rate for the measurement, C = total count, and B = total background count. The standard deviation in the net intensity is given by $\sigma^2(I) = (K/\text{NPI})^2[C + 4B + (pI)^2]$, where p is a factor used to downweight intense reflections. The observed structure factor amplitude F_o is given by $F_o = (I/Lp)^{1/2}$, where Lp = Lorentz and polarization factors. The $\sigma(I)$'s were converted to the estimated errors in the relative structure factors $\sigma(F_o)$ by $\sigma(F_o) = {}^1/_2(\sigma(I)/I)F_o$.

(19) The function minimized was $\sum w(|F_o| - |F_c|)^2$, where $w = 1/\sigma^2(F_o)$. The unweighted and weighted residuals are defined as $R = (\sum||F_o| - |F_c||)/\sum|F_o|$ and $R_w = [(\sum w(|F_o| - |F_c|))^2/(\sum w|F_o|)^2]^{1/2}$. The error in an observation of unit weight is $[\sum w(|F_o| - |F_c|)^2/(\text{NO} - \text{NV})]^{1/2}$, where NO and NV are the number of observations and variables, respectively.

(20) Cromer, D. T.; Waber, J. T. "International Tables for X-ray Crystallography"; Kynoch Press: Birmingham, England, 1974; Vol. IV, Table 2.2.4. Cromer, D. T. *Ibid.*, Table 2.3.1.

(21) Cromer, D. T.; Ibers, J. A. "International Tables for X-ray Crystallography"; Kynoch Press: Birmingham, England, 1974; Vol. IV.

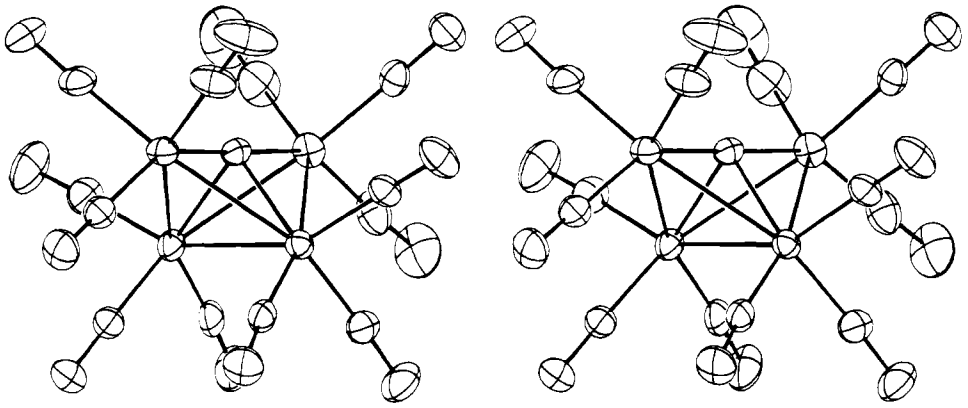

Figure 1. Stereoview of $[Fe_4N(CO)_{12}]^-$.

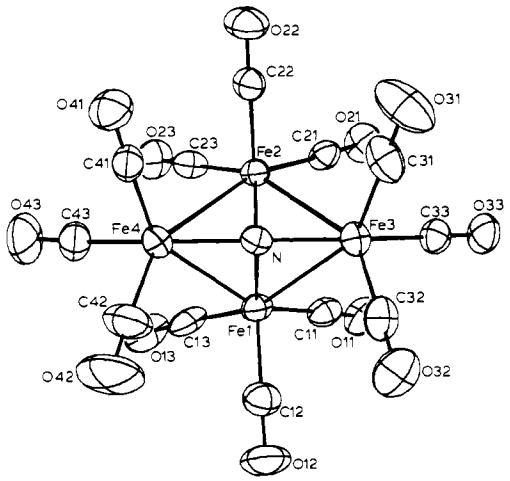

Figure 2. Perspective view looking down the pseudo-C_2 axis showing the atom labels.

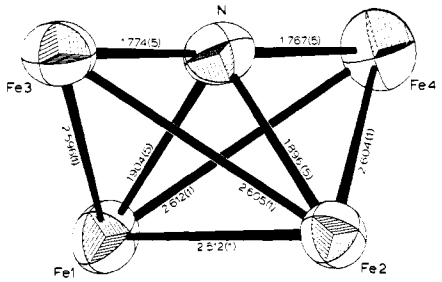

Figure 3. View showing the Fe_4N framework with bond distances in Å.

that the twist itself is not symmetric.

The core of the cluster consists of an Fe_4N unit. Initially, the most striking features of this moiety is the Fe(3)–N–Fe(4) angle of 179.0 (3)°. The interactions between Fe(3)–N and Fe(4)–N are the same, as seen in Figure 3, but these distances are 0.130 (5) Å shorter than the equivalent Fe(1)–N and Fe(2)–N distances. The coordination geometry about the nitrogen atom is close to octahedral with two vacant sites. The only deviation is seen in the Fe(1)–N–Fe(2) angle of 82.8 (2)°. The Fe–Fe distances between the wing-tip atoms (3 and 4) and the hinge atoms are essentially the same and average 2.604 (7) Å. The unique Fe(1)–Fe(2) distance is 0.092 Å shorter than the others. The dihedral angle between the planes comprised of Fe(3)–Fe(1)–Fe(2) and Fe(4)–Fe(1)–Fe(2) is 78.2°.

The ligands are all ordered linear carbonyls, exhibiting no unusual distances or angles. One feature does deserve comment. The unique carbonyls on Fe(3) and Fe(4) (C(33)–O(33) and C(43)–O(43)) have slightly longer Fe–C distances than the remaining ligands. The average of all the Fe–C distances except these is 1.78 (1) Å, whereas Fe(3)–C(33) and Fe(4)–C(43) are 1.811 (8) and 1.815 (9) Å, respectively.

Discussion

The Butterfly Structure. $PPN[Fe_4N(CO)_{12}]$ contains four iron atoms in the so-called butterfly arrangement. Recently, several compounds having just one atom in the bridging position of the type described here have been reported.[2,3,22,23] $[Fe_4(CO)_{13}H]^{3-}$ is one example where the bridging ligand is a CO bound in the μ_4-η^2 manner shown in III. Included in

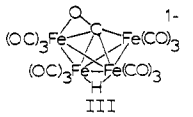

III

this group are $Fe_4(CO)_{12}(CCO_2CH_3)$,[22] $Fe_4(CH)(CO)_{12}H$,[2] $[Fe_4C(CO)_{12}]^{2-}$,[2] and $Fe_4(CO)_{12}(COCH_3)H$.[23] A second series of butterfly structures have also emerged containing a bridging ligand which interacts only with the wing-tip metals. Two examples containing μ_2 ligands are $[Ru_4Cl(CO)_{13}]^-$[24] (IV) and $Os_4(OH)(CO)_{12}H_3$[25] (V).

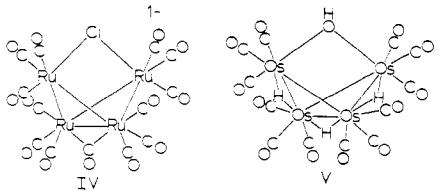

IV V

The underlying reason for adoption of the butterfly arrangement has been approached theoretically[26] and results from the lowering of a high-energy antibonding molecular orbital compared to the molecular orbital diagram of the tetrahedral arrangement and requires 62 electrons for its stable configuration. The μ_4 bridging atom(s) such as the N in $[Fe_4N(CO)_{12}]^-$ or CH in $Fe_4(CH)(CO)_{12}H$ contribute five electrons to the cluster while those ligands bridging only the wing-tip metals contribute three electrons. The difference of two electrons is supplemented by an additional carbon monoxide in $[Ru_4Cl(CO)_{13}]^-$ or two hydrogens in $Os_4(OH)(CO)_{12}H_3$ to attain the 62-electron configuration. The existence

(22) Bradley, J. S.; Ansell, G. B.; Hill, E. W. *J. Am. Chem. Soc.* **1979**, *101*, 7417–7419.
(23) Holt, E. M.; Whitmire, K.; Shriver, D. F. *J. Chem. Soc., Chem. Commun.* **1980**, 778–779.
(24) Steinmetz, G. R.; Harley, A. D.; Geoffroy, G. L. *Inorg. Chem.* **1980**, *19*, 2985–2989.
(25) Johnson, B. F. G.; Lewis, J.; Raithby, P. R.; Zuccaro, C. *J. Chem. Soc., Dalton Trans.* **1980**, 716–720.
(26) Lauher, J. W. *J. Am. Chem. Soc.* **1978**, *100*, 5305–5315.

Table II. Positional and Thermal Parameters and Their Estimated Standard Deviations for PPN[$Fe_4N(CO)_{12}$][a]

atom	x	y	z	B(1,1)	B(2,2)	B(3,3)	B(1,2)	B(1,3)	B(2,3)
Fe(1)	0.1824 (1)	0.28868 (8)	0.78104 (7)	0.0084 (1)	0.00621 (7)	0.00377 (5)	0.0004 (2)	−0.0003 (1)	0.00229 (10)
Fe(2)	0.0897 (1)	0.37745 (8)	0.66378 (6)	0.0094 (1)	0.00458 (6)	0.00334 (4)	0.0023 (1)	0.0002 (1)	0.00024 (9)
Fe(3)	−0.0619 (1)	0.27197 (8)	0.75294 (7)	0.0084 (1)	0.00516 (6)	0.00452 (5)	0.0002 (1)	0.0010 (1)	−0.00091 (10)
Fe(4)	0.1814 (1)	0.22067 (8)	0.63029 (7)	0.0108 (1)	0.00604 (7)	0.00452 (5)	0.0059 (2)	0.0015 (1)	0.00033 (10)
P(1)	0.7060 (2)	0.7298 (1)	0.8123 (1)	0.0071 (2)	0.0037 (1)	0.00311 (7)	0.0017 (2)	0.0007 (2)	−0.0000 (1)
P(2)	0.6022 (2)	0.9045 (1)	0.7510 (1)	0.0086 (2)	0.0036 (1)	0.00408 (9)	0.0008 (2)	−0.0006 (2)	0.0003 (2)
O(11)	0.1532 (6)	0.4291 (4)	0.9106 (3)	0.0166 (8)	0.0094 (4)	0.0047 (3)	−0.0035 (10)	−0.0003 (8)	−0.0020 (6)
O(12)	0.2098 (7)	0.1234 (5)	0.8843 (4)	0.0215 (10)	0.0120 (5)	0.0092 (4)	0.0067 (11)	0.0006 (10)	0.0130 (6)
O(13)	0.4516 (5)	0.3519 (5)	0.7713 (4)	0.0102 (7)	0.0179 (6)	0.0062 (3)	−0.0075 (11)	−0.0013 (8)	0.0065 (7)
O(21)	0.0150 (6)	0.5432 (4)	0.7477 (4)	0.0245 (9)	0.0055 (3)	0.0068 (3)	0.0079 (9)	0.0060 (9)	−0.0025 (5)
O(22)	−0.0687 (6)	0.3887 (4)	0.5089 (3)	0.0182 (8)	0.0104 (4)	0.0050 (3)	0.0097 (10)	−0.0068 (8)	−0.0018 (6)
O(23)	0.3248 (5)	0.4889 (4)	0.6220 (4)	0.0125 (7)	0.0101 (5)	0.0081 (3)	−0.0043 (10)	0.0052 (8)	0.0038 (7)
O(31)	−0.2881 (6)	0.2568 (5)	0.6381 (5)	0.0162 (8)	0.0113 (5)	0.0139 (5)	0.0068 (11)	−0.0149 (10)	−0.0093 (9)
O(32)	−0.1114 (6)	0.0928 (4)	0.8388 (4)	0.0187 (9)	0.0074 (4)	0.0088 (4)	−0.0061 (10)	0.0052 (9)	0.0027 (7)
O(33)	−0.1589 (6)	0.4013 (4)	0.8699 (3)	0.0180 (8)	0.0081 (4)	0.0058 (3)	0.0071 (9)	0.0066 (7)	−0.0014 (6)
O(41)	0.0477 (6)	0.1807 (4)	0.4674 (3)	0.0181 (8)	0.0088 (4)	0.0051 (3)	0.0044 (10)	−0.0005 (8)	−0.0013 (6)
O(42)	0.2182 (10)	0.0283 (5)	0.6712 (5)	0.0564 (17)	0.0095 (5)	0.0114 (5)	0.0311 (13)	−0.0012 (16)	0.0050 (8)
O(43)	0.4328 (6)	0.2802 (6)	0.5710 (4)	0.0119 (7)	0.0200 (8)	0.0099 (4)	0.0074 (13)	0.0085 (9)	0.0006 (10)
N(2)	0.6935 (5)	0.8329 (4)	0.7806 (3)	0.0087 (6)	0.0037 (3)	0.0044 (3)	0.0012 (8)	−0.0004 (7)	−0.0001 (5)
N	0.0605 (5)	0.2473 (4)	0.6915 (3)	0.0082 (6)	0.0041 (3)	0.0041 (3)	0.0008 (8)	−0.0001 (7)	0.0007 (5)
C(11)	0.1601 (7)	0.3732 (6)	0.8595 (5)	0.0106 (9)	0.0074 (5)	0.0040 (3)	−0.002 (1)	−0.002 (1)	0.0014 (7)
C(12)	0.1978 (8)	0.1863 (6)	0.8430 (5)	0.0116 (10)	0.0082 (6)	0.0058 (4)	0.002 (1)	−0.001 (1)	0.0022 (9)
C(13)	0.3446 (8)	0.3265 (6)	0.7720 (4)	0.0135 (10)	0.0099 (6)	0.0030 (3)	−0.002 (1)	−0.002 (1)	0.0032 (8)
C(21)	0.0404 (8)	0.4758 (5)	0.7170 (4)	0.0144 (10)	0.0049 (5)	0.0039 (3)	0.003 (1)	0.003 (1)	0.0014 (7)
C(22)	−0.0062 (7)	0.3828 (5)	0.5689 (5)	0.0117 (9)	0.0056 (5)	0.0043 (4)	0.004 (1)	−0.000 (1)	−0.0012 (7)
C(23)	0.2342 (7)	0.4433 (6)	0.6368 (5)	0.0109 (9)	0.0061 (5)	0.0049 (4)	0.002 (1)	−0.002 (1)	0.0019 (8)
C(31)	−0.2005 (8)	0.2625 (6)	0.6829 (6)	0.0123 (10)	0.0074 (6)	0.0081 (5)	0.004 (1)	0.000 (1)	−0.0060 (9)
C(32)	−0.0930 (7)	0.1633 (6)	0.8066 (5)	0.0093 (9)	0.0069 (6)	0.0064 (4)	−0.003 (1)	0.003 (1)	−0.0020 (8)
C(33)	−0.1201 (7)	0.3511 (6)	0.8256 (5)	0.0103 (9)	0.0067 (5)	0.0047 (4)	0.001 (1)	0.002 (1)	−0.0001 (8)
C(41)	0.1017 (7)	0.1955 (6)	0.5299 (5)	0.0121 (9)	0.0064 (5)	0.0049 (4)	0.005 (1)	0.005 (1)	0.0014 (7)
C(42)	0.2083 (10)	0.1043 (7)	0.6556 (6)	0.0229 (14)	0.0088 (7)	0.0072 (5)	0.013 (2)	−0.004 (1)	0.0018 (10)
C(43)	0.3371 (8)	0.2570 (7)	0.5956 (5)	0.0132 (10)	0.0123 (8)	0.0051 (4)	0.008 (1)	0.003 (1)	−0.0007 (10)

atom	x	y	z	B_{iso}, Å^2	atom	x	y	z	B_{iso}, Å^2
C1A	0.5837 (6)	0.6818 (5)	0.8755 (4)	3.0 (1)	C4F	0.7593 (9)	1.0638 (7)	0.5356 (6)	7.0 (2)
C2A	0.6060 (7)	0.6706 (5)	0.9597 (4)	4.0 (2)	C5F	0.8427 (9)	1.0190 (6)	0.5857 (5)	6.5 (2)
C3A	0.5104 (7)	0.6330 (5)	1.0056 (5)	4.5 (2)	C6F	0.7903 (7)	0.9688 (6)	0.6525 (5)	5.0 (2)
C4A	0.3904 (7)	0.6073 (6)	0.9688 (5)	4.9 (2)	H2A	0.6919 (0)	0.6907 (0)	0.9868 (0)	4.1000 (0)
C5A	0.3646 (7)	0.6179 (6)	0.8869 (5)	4.9 (2)	H3A	0.5255 (0)	0.6253 (0)	1.0646 (0)	4.4000 (0)
C6A	0.4609 (7)	0.6548 (5)	0.8395 (4)	4.1 (2)	H4A	0.3235 (0)	0.5807 (0)	1.0025 (0)	5.6000 (0)
C1B	0.7048 (6)	0.6443 (5)	0.7287 (4)	3.1 (1)	H5A	0.2793 (0)	0.6006 (0)	0.8621 (0)	5.9000 (0)
C2B	0.7578 (8)	0.6761 (6)	0.6572 (5)	5.2 (2)	H6A	0.4420 (0)	0.6610 (0)	0.7803 (0)	5.0000 (0)
C3B	0.7610 (8)	0.6096 (6)	0.5924 (5)	6.2 (2)	H2B	0.7939 (0)	0.7432 (0)	0.6531 (0)	5.9000 (0)
C4B	0.7073 (8)	0.5165 (6)	0.5970 (5)	5.4 (2)	H3B	0.7559 (0)	0.6346 (0)	0.5360 (0)	7.1000 (0)
C5B	0.6582 (8)	0.4865 (6)	0.6683 (5)	5.2 (2)	H4B	0.8242 (0)	0.4780 (0)	0.5718 (0)	6.4000 (0)
C6B	0.6570 (7)	0.5501 (5)	0.7346 (4)	4.3 (2)	H5B	0.5972 (0)	0.4276 (0)	0.6613 (0)	6.0000 (0)
C1C	0.8554 (6)	0.7358 (5)	0.8724 (4)	3.3 (1)	H6B	0.6235 (0)	0.5277 (0)	0.7869 (0)	5.2000 (0)
C2C	0.9185 (8)	0.8243 (6)	0.8989 (5)	5.2 (2)	H2C	0.8848 (0)	0.8840 (0)	0.8840 (0)	6.2000 (0)
C3C	1.0335 (9)	0.8288 (7)	0.9480 (5)	6.4 (2)	H3C	1.0798 (0)	0.8896 (0)	0.9688 (0)	7.7000 (0)
C4C	1.0800 (8)	0.7474 (6)	0.9677 (5)	6.1 (2)	H4C	1.1606 (0)	0.7516 (0)	1.0023 (0)	7.0000 (0)
C5C	1.0206 (8)	0.6604 (6)	0.9418 (5)	5.4 (2)	H5C	1.0598 (0)	0.6033 (0)	0.9570 (0)	6.4000 (0)
C6C	0.9052 (7)	0.6546 (5)	0.8934 (4)	4.2 (2)	H6C	0.8601 (0)	0.5927 (0)	0.8748 (0)	5.5000 (0)
C1D	0.4449 (7)	0.8501 (5)	0.7178 (4)	3.9 (2)	H2D	0.5020 (0)	0.7839 (0)	0.6147 (0)	5.8000 (0)
C2D	0.4301 (8)	0.7905 (6)	0.6474 (5)	5.2 (2)	H3D	0.2928 (0)	0.6987 (0)	0.5741 (0)	7.0000 (0)
C3D	0.3081 (9)	0.7388 (6)	0.6240 (6)	6.4 (2)	H4D	0.1343 (0)	0.7114 (0)	0.6527 (0)	7.5000 (0)
C4D	0.2149 (9)	0.7490 (7)	0.6702 (6)	6.8 (2)	H5D	0.1512 (0)	0.8082 (0)	0.7700 (0)	7.5000 (0)
C5D	0.2245 (9)	0.8045 (7)	0.7397 (6)	6.8 (2)	H6D	0.3553 (0)	0.8987 (0)	0.8156 (0)	6.7000 (0)
C6D	0.3446 (8)	0.8581 (6)	0.7643 (5)	5.5 (2)	H2E	0.5243 (0)	1.0965 (0)	0.7612 (0)	7.4000 (0)
C1E	0.5954 (7)	0.9912 (5)	0.8337 (4)	3.8 (2)	H3E	0.5260 (0)	1.2070 (0)	0.8755 (0)	7.4000 (0)
C2E	0.5536 (9)	1.0795 (6)	0.8171 (5)	6.4 (2)	H4E	0.6028 (0)	1.1738 (0)	1.0058 (0)	7.0000 (0)
C3E	0.5586 (9)	1.1458 (7)	0.8839 (6)	6.8 (2)	H5E	0.6693 (0)	1.0281 (0)	1.0334 (0)	6.3000 (0)
C4E	0.6012 (8)	1.1261 (6)	0.9604 (5)	6.0 (2)	H6E	0.6683 (0)	0.9127 (0)	0.9243 (0)	5.7000 (0)
C5E	0.6405 (8)	1.0423 (6)	0.9765 (5)	5.6 (2)	H2F	0.4965 (0)	1.0169 (0)	0.6246 (0)	6.4000 (0)
C6E	0.6388 (7)	0.9740 (5)	0.9127 (5)	4.5 (2)	H3F	0.5863 (0)	1.1009 (0)	0.5090 (0)	7.9000 (0)
C1F	0.6652 (7)	0.9667 (5)	0.6646 (4)	4.1 (2)	H4F	0.7945 (0)	1.0959 (0)	0.4883 (0)	7.7000 (0)
C2F	0.5867 (8)	1.0158 (6)	0.6131 (5)	5.8 (2)	H5F	0.9330 (0)	1.0206 (0)	0.5759 (0)	7.4000 (0)
C3F	0.6380 (9)	1.0658 (7)	0.5475 (6)	6.7 (2)	H6F	0.8450 (0)	0.9368 (0)	0.6921 (0)	5.6000 (0)

[a] The form of the anisotropic thermal parameter is $\exp[-(B(1,1)h^2 + B(2,2)k^2 + B(3,3)l^2 + B(1,2)hk + B(1,3)hl + B(2,3)kl)]$.

of two such closely related structural types suggests that it may be possible for an interconversion between the two bridging forms (μ_4 and μ_2) to occur. We are currently exploring the chemistry of these derivatives in light of this possibility.

The requirement for nitrogen to be a five-electron donor offers some rationale regarding the site of protonation; this occurs on the iron atoms rather than on the nitrogen. In other words, the normally available lone pair must be in some fashion donated to the cluster. The simplest explanation would involve an interaction with a vacant metal orbital trans to the unique carbonyl on each of the wing-tip iron atoms. This type of π-interaction increases the net bonding between the N and the

Table III. Bond Distances

atoms	dist, Å	atoms	dist, Å
Fe(1)-Fe(2)	2.512 (1)	Fe(4)-C(42)	1.760 (9)
Fe(1)-Fe(3)	2.596 (1)	Fe(4)-C(43)	1.815 (9)
Fe(1)-Fe(4)	2.612 (1)	C(11)-O(11)	1.148 (8)
Fe(2)-Fe(3)	2.605 (1)	C(12)-O(12)	1.141 (8)
Fe(2)-Fe(4)	2.604 (1)	C(13)-O(13)	1.155 (8)
Fe(3)-Fe(4)	3.541 (1)	C(21)-O(21)	1.142 (7)
N-Fe(1)	1.904 (5)	C(22)-O(22)	1.149 (7)
N-Fe(2)	1.896 (5)	C(23)-O(23)	1.137 (7)
N-Fe(3)	1.774 (5)	C(31)-O(31)	1.134 (8)
N-Fe(4)	1.767 (5)	C(32)-O(32)	1.137 (8)
Fe(1)-C(11)	1.782 (8)	C(33)-O(33)	1.140 (7)
Fe(1)-C(12)	1.798 (8)	C(41)-O(41)	1.130 (9)
Fe(1)-C(13)	1.767 (8)	C(42)-O(42)	1.125 (9)
Fe(2)-C(21)	1.782 (7)	C(43)-O(43)	1.139 (8)
Fe(2)-C(22)	1.791 (7)	C-C_{av}	1.38 (3)
Fe(2)-C(23)	1.788 (7)	P(1)-C_{av}	1.798 (6)
Fe(3)-C(31)	1.785 (9)	P(2)-C_{av}	1.803 (10)
Fe(3)-C(32)	1.789 (8)	P(1)-N(2)	1.575 (5)
Fe(3)-C(33)	1.811 (8)	P(2)-N(2)	1.555 (5)
Fe(4)-C(41)	1.786 (8)		

Table IV. Selected Bond Angles

atoms	angle, deg	atoms	angle, deg
Fe(2)-Fe(1)-Fe(4)	61.04 (3)	C(31)-Fe(3)-C(32)	100.1 (4)
Fe(3)-Fe(1)-Fe(4)	85.64 (4)	C(31)-Fe(3)-C(33)	94.5 (3)
Fe(2)-Fe(1)-N	48.5 (1)	C(32)-Fe(3)-C(33)	98.3 (3)
Fe(3)-Fe(1)-N	43.1 (2)	Fe(1)-N-Fe(2)	82.8 (2)
Fe(2)-Fe(1)-C(11)	95.4 (2)	Fe(1)-N-Fe(3)	89.8 (2)
Fe(2)-Fe(1)-C(12)	154.9 (2)	Fe(1)-N-Fe(4)	90.7 (2)
Fe(2)-Fe(1)-C(13)	99.2 (2)	Fe(2)-N-Fe(3)	90.4 (2)
Fe(3)-Fe(1)-C(11)	84.7 (2)	Fe(2)-N-Fe(4)	90.5 (2)
Fe(3)-Fe(1)-C(12)	100.3 (2)	Fe(3)-N-Fe(4)	179.0 (3)
Fe(3)-Fe(1)-C(13)	160.5 (2)	Fe(1)-C(11)-O(11)	176.1 (7)
Fe(4)-Fe(1)-C(11)	156.3 (2)	Fe(1)-C(12)-O(12)	177.7 (7)
Fe(4)-Fe(1)-C(12)	103.2 (3)	Fe(1)-C(13)-O(13)	175.8 (6)
Fe(4)-Fe(1)-C(13)	85.0 (2)	Fe(2)-C(21)-O(21)	174.8 (6)
N-Fe(1)-C(11)	124.1 (3)	Fe(2)-C(22)-O(22)	178.1 (7)
N-Fe(1)-C(12)	106.5 (3)	Fe(2)-C(23)-O(23)	176.6 (7)
N-Fe(1)-C(13)	125.2 (3)	Fe(3)-C(31)-O(31)	179.6 (8)
C(11)-Fe(1)-C(12)	99.8 (3)	Fe(3)-C(32)-O(32)	177.9 (7)
C(11)-Fe(1)-C(13)	97.4 (3)	Fe(3)-C(33)-O(33)	178.4 (7)
C(12)-Fe(1)-C(13)	98.5 (3)	Fe(4)-C(41)-O(41)	177.7 (7)
Fe(1)-Fe(3)-Fe(2)	57.77 (3)	Fe(4)-C(42)-O(42)	176 (1)
Fe(1)-Fe(3)-N	47.2 (2)	Fe(4)-C(43)-O(43)	177.4 (8)
Fe(1)-Fe(3)-C(31)	150.7 (3)	P(1)-N(2)-P(2)	146.5 (3)
Fe(1)-Fe(3)-C(32)	95.7 (2)	C-P(1)-C (av)	107 (1)
Fe(1)-Fe(3)-C(33)	107.6 (2)	C-P(2)-C (av)	108 (1)
Fe(2)-Fe(3)-C(31)	97.8 (3)	C-P(1)-N(2) (av)	111 (4)
Fe(2)-Fe(3)-C(32)	147.4 (2)	C-P(2)-N(2) (av)	111 (3)
Fe(2)-Fe(3)-C(33)	107.2 (2)	P(1)-C-C (av)	120 (2)
N-Fe(3)-C(31)	104.9 (3)	P(2)-C-C (av)	120 (1)
N-Fe(3)-C(32)	102.1 (3)	C-C-C (av)	120 (2)
N-Fe(3)-C(33)	148.7 (3)		

Table V. Stoichiometry of Reaction 1: Synthesis of PPN[$Fe_4N(CO)_{12}$]

$Fe_3(CO)_{12}$, mmol	$Fe(CO)_3(NO)^-$, mmol	$Fe(CO)_5$,[a] mmol	$Fe_3(CO)_{12}$/ $Fe(CO)_3(NO)^-$	$Fe(CO)_5$/ $Fe(CO)_3(NO)^-$
0.462	0.291	0.424	1.59	1.46
0.439	0.291	0.420	1.51	1.44
0.583[b]	0.291	0.427	2.00	1.45
0.454	0.463[b]	0.412	0.98	0.89

[a] Determined by its electronic absorption spectrum after distillation of solvent and $Fe(CO)_5$ into a separate vessel. [b] Unreacted starting material remained as observed by infrared spectroscopy.

wing-tip irons, which is clearly reflected in the shortened Fe–N distances of the atoms and may also help explain the observable increase in the Fe(3)–C(33) and Fe(4)–C(43) bond distances of 0.03 Å.

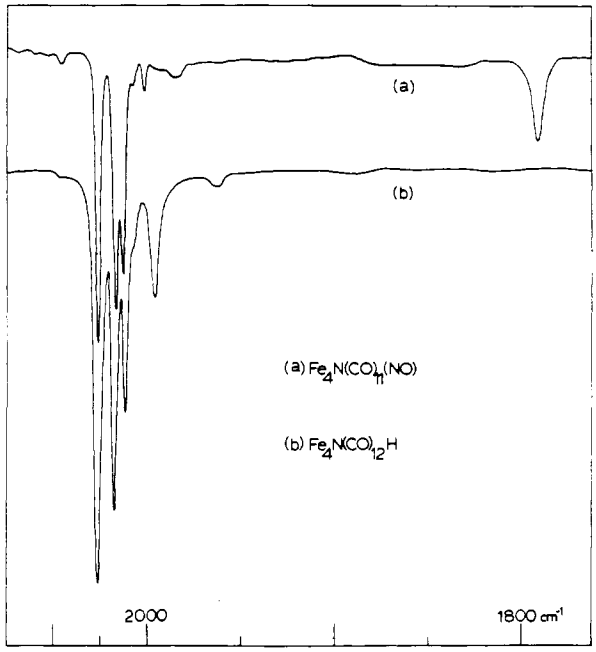

Figure 4. Comparison of the carbonyl and nitrosyl region infrared spectra of $Fe_4N(CO)_{11}(NO)$ and $Fe_4N(CO)_{12}H$ in hexane.

Synthesis and Reactivity. Our original goal in reacting $[Fe(CO)_3NO]^-$ with $Fe_3(CO)_{12}$ was to prepare the nitrosyl carbonyl cluster $[Fe_4(CO)_{12}NO]^-$. Our basis for attempting this reaction was the result obtained in similar work with $Ru_3(CO)_{12}$ in which the tetrahedral cluster $[FeRu_3(CO)_{12}N-O]^-$ (VI) was prepared in high yield.[9] The stoichiometry of

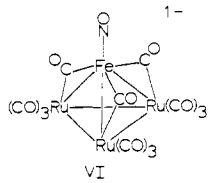

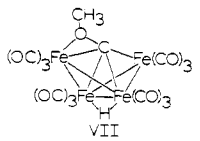

the reaction forming $[Fe_4N(CO)_{12}]^-$ (eq 1) is indicative of the complexity of the mechanism. Although $[FeRu_3(CO)_{12}NO]^-$ is the only product resulting from the reaction of $Ru_3(CO)_{12}$ with $[Fe(CO)_3NO]^-$, we found no evidence for the intermediacy of the analogous compound $[Fe_4(CO)_{12}(NO)]^-$ in the current study. The chemistry of some isoelectronic analogues of $[Fe_4(CO)_{12}NO]^-$ discussed above may be relevant in our attempt to rationalize this fact. When tetrahedral $[Fe_4(CO)_{13}]^{2-}$ is protonated, the product $[HFe_4(CO)_{13}]^-$ has a unique butterfly structure[3] (III). Recently $[Fe_4(CO)_{13}]^{2-}$ was methylated,[27,28] giving the tetrahedral cluster $[Fe_4(CO)_{12}(C-OCH_3)]^-$, which upon protonation converts into a butterfly arrangement having a (μ_4-η^2-$COCH_3$) ligand[23] (VII). It is possible that a similar butterfly structure could exist with $[Fe_4(CO)_{12}NO]^-$ (VIII), and that this may activate the oxygen

bound to the nitrogen. Migratory insertion of a coordinated CO into the Fe–O bond followed by elimination of CO_2 would give the unsaturated metal nitride that would trap a CO from the atmosphere (CO is displaced in the initial stages of Fe–Fe

(27) Whitmire, K.; Shriver, D. F.; Holt, E. M. *J. Chem. Soc., Chem. Commun.* **1980**, 780–781.
(28) Dawson, P. A.; Johnson, B. F. G.; Lewis, J.; Raithby, P. R. *J. Chem. Soc., Chem. Commun.* **1980**, 781–783.

Table VI. Spectroscopic Data

cluster	color	λ_{max}, nm	δ	ν_{CO}, cm^{-1}
$[PPN][Fe_4N(CO)_{12}]$	brown	293, 575	+7.8 (acetone-d_6)	2016 s, 1991 vs, 1966 m, 1933 w (THF)
$Fe_4N(CO)_{12}H$	red-brown	288, 575	−31.2 ($CDCl_3$)	2054 vs, 2035 s, 2024 s, 2015 w (sh), 1987 m, 1961 w (hexane)
$Fe_4N(CO)_{11}(NO)$	brown	299		2094 w, 2054 vs, 2036 s, 2029 s, 2017 w, 2006 m [ν_{NO} 1789 m] (hexane)
$Fe_3(CO)_{10}(NH)$	red	290, 462	+9.5 ($J_{^{14}N-^1H}$ = 57 Hz, $CDCl_3$)	2094 w, 2051 vs, 2025 s, 1998 m, 1749 m (hexane) (ν_{NH}; $CHCl_3$: 3368)
$Fe_3(CO)_{10}(NSi(CH_3)_3)$[31]	red			2088 w, 2048 vs, 2020 s, 2014 s, 1993 m, 1743 s (hexane)
$Fe_3(CO)_9(NH)_2$	red	304, 498	+5.3 ($CDCl_3$)	2091 w, 2053 s, 2035 s, 2009 s (hexane), 1992 m
$Fe_3(CO)_9(NCH_2CH_3)(NH)$[32]	red		1.22 (CH_3), 3.32 (CH_2), 3.77 (N-H) ($CDCl_3$)	2051 vs, 2031 vs, 2005 s, 1988 m (hexane)

bond formation). It is also possible that such an activation of the oxygen atom may result in it becoming more nucleophilic and attacking an additional $Fe_3(CO)_{12}$.

In the syntheses of nitrido clusters involving the nitrosonium ion, it is very likely that the reactions proceed via an intermediate metal nitrosyl. Two nitrosyl carbonyl clusters have been prepared by this reaction. $Ru_3(CO)_{10}(NO)H$ was synthesized[29] by the reaction of $[Ru_3(CO)_{11}H]^-$ with NO^+, and in this study we have found that $[Fe_4N(CO)_{12}]^-$ reacts with NO^+ to give $Fe_4N(CO)_{11}(NO)$. Although the current study represents the first direct observation of a coordinated nitrosyl being deoxygenated to the nitride with low-valent metals, the reaction has been observed with metals in high oxidation states. The compound $K_3[Ru_2NCl_8(H_2O)_2]$, which has a linear Ru–N–Ru linkage, can be synthesized by the action of reducing agents such as $SnCl_2$ or formaldehyde on $K_2[RuCl_5(NO)]$.[30]

This conversion of a coordinated nitrosyl into a nitride may have some relevance to the surface-catalyzed oxidation of CO with 2NO to give CO_2 and N_2O. In effect, we have conducted the first stage of this reaction (eq 2), and it now remains for

$$(M)\text{–}CO + (M)\text{–}NO \rightarrow (M)\text{–}N + CO_2(g) \qquad (2)$$

us to observe the second stage (eq 3).

$$(M)\text{–}N + (M)\text{–}NO \rightarrow N_2O(g) \qquad (3)$$

The compound which has been identified as $Fe_4N(CO)_{11}(NO)$ is particularly interesting in this light because it apparently contains both of the functional groups on the left side of eq 3. Unfortunately, we have not been able to obtain crystals of $Fe_4N(CO)_{11}(NO)$ suitable for X-ray crystallography. Although the infrared (Figure 4) and UV–visible spectral similarities to those of $Fe_4N(CO)_{12}H$ would suggest a structure such as IX, a closed tetrahedral arrangement such

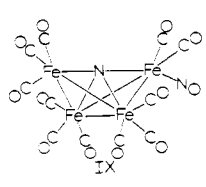

IX

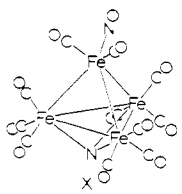

X

as X is also possible. Further work is in progress to determine the structure and reactivity of this nitrosyl nitrido cluster.

Another surface-catalyzed reaction which also proceeds via a nitride intermediate is the hydrogenation of N_2. Extensive studies have shown that N_2 is dissociatively adsorbed on an iron surface and subsequently forms three N–H bonds from surface-adsorbed H atoms.[13] Two of the products obtained from the aqueous protonation of $Na[Fe_4N(CO)_{12}]$ have bridging imido groups. The evidence supporting the assignment of XI to the structure of $Fe_3(NH)(CO)_{10}$ and XII to the

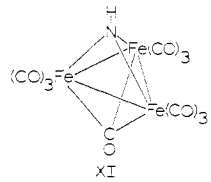

XI

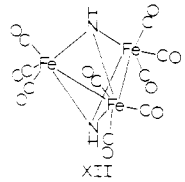

XII

structure of $Fe_3(NH)_2(CO)_9$ derives from a comparison of the infrared spectra to structurally characterized analogues. In the case of $Fe_3(NH)(CO)_{10}$, an identical compound where a trimethylsilyl group was bound to the nitrogen has been prepared.[31] The similarity in the infrared spectra of these two species suggests they are isostructural. Convincing evidence that an N–H bond is present comes from the ^1H NMR spectrum which shows a $J_{^{14}N-^1H}$ of 57 Hz. This value is similar to that of NH_3 and is in the range normal for pyramidal N compounds. The fact that observation of this signal is possible at all is indicative of a relatively high symmetry around nitrogen. The case for $Fe_3(NH)_2(CO)_9$ is much less sound because of the minute quantities that have been isolated. The formulation is similar to the compound $Fe_3(NEt)(NH)(CO)_9$ which has been characterized.[32]

Although infrared evidence suggests that $Na[Fe_4N(CO)_{12}]$ is the only species present prior to protonation, the conditions of aqueous protonation may affect side reactions such that the three minor products, $Fe_4N(CO)_{11}(NO)$, $Fe_3(NH)(CO)_{10}$, and $Fe_3(NH)_2(CO)_9$, need not be derived from the same immediate precursor. At this stage we find these transformations intriguing but offer no explanation for their formation. Further work within this iron system, particularly among these minor products, may shed light on their formation and importantly on the step in which the N–H bond is formed.

Acknowledgment is made to the donors of the Petroleum Research Fund, administered by the American Chemical Society, for support of this research, and to DuPont Corp. for a Young Faculty Research Grant. We also gratefully acknowledge L. H. Pignolet and M. McGuiggan for assistance in the structural analyses and the NSF for partial support of our X-ray diffraction and structure-solving equipment (NSF Grant CHE77-28505).

Registry No. $PPN[Fe_4N(CO)_{12}]$, 76791-99-6; $Na[Fe_4N(CO)_{12}]$, 76791-98-5; $Fe_4N(CO)_{11}(NO)$, 78571-88-7; $Fe_3(NH)_2(CO)_9$, 78571-89-8; $Fe_3(NH)(CO)_{10}$, 77456-69-0; $PPN[Fe(CO)_3(NO)]$, 61003-17-6; $Fe_3(CO)_{12}$, 17685-52-8; $Na[Fe(CO)_3(NO)]$, 25875-18-7; $NOPF_6$, 16921-91-8.

Supplementary Material Available: A listing of the structure factors derived from the crystallographic analysis (18 pages). Ordering information is given on any current masthead page.

(29) Johnson, B. F. G.; Raithby, P. R.; Zuccaro, C. *J. Chem. Soc., Dalton Trans.* **1980**, 99–104.
(30) Brizard, L. *C. R. Hebd. Seances Acad. Sci.* **1896**, *123*, 182; *Ann. Chim. Phys.* **1900**, [7]*21*, 311. Cleare, M. J.; Griffith, W. P. *J. Chem. Soc. A* **1970**, 1117.
(31) (a) Koerner von Gustorf, E.; Wagner, R. *Angew. Chem., Int. Ed. Engl.* **1971**, *10*, 910. (b) Barnett, B. L.; Kruger, C. *Ibid.* **1971**, *10*, 910–911.
(32) Aime, S.; Gervasio, G.; Milone, L.; Rossetti, R.; Stanghellini, P. L. *J. Chem. Soc., Dalton Trans.* **1978**, 534–540.